American Mineralogist, Volume 91, pages 1888–1892, 2006

A high-pressure Raman spectroscopic study of hafnon, $HfSiO_4$

Bouchaib Manoun,[1,*] Robert T. Downs,[2] and Surendra K. Saxena[1]

[1]Center for the Study of Matter at Extreme Conditions, Florida International University, U.P., VH-140, Miami, Florida 33199, U.S.A.
[2]Department of Geosciences, University of Arizona, 1040 E 4th Street, Tucson, Arizona 85721-0077, U.S.A.

Abstract

Raman spectra of synthetic $HfSiO_4$ were determined to pressures of 38.2 GPa. Changes in the spectra indicate that $HfSiO_4$ undergoes a room-temperature phase transition from the hafnon structure ($I4_1/amd$ space group) to the scheelite structure ($I4_1/a$ space group) at a pressure of ~19.6 GPa. Upon release of pressure to ambient conditions, the spectra indicate that the sample retains the scheelite structure. Zircon has been classified previously as the least compressible tetrahedrally coordinated silicate known. However, pressure derivatives of the peak positions in hafnon are smaller than those in zircon, and suggest that hafnon is more incompressible than zircon. Furthermore, the pressure derivatives also suggest that the high-pressure, scheelite-structured $HfSiO_4$ phase is more incompressible than the scheelite-structured $ZrSiO_4$ (reidite). Thus, the post-hafnon phase appears to be even more incompressible than hafnon, which would make it the least compressible tetrahedrally coordinated silicate known to date.

Keywords: Raman Spectroscopy, hafnon, phase transformation, scheelite-structured $HfSiO_4$

Introduction

Hafnon is the naturally occurring phase of hafnium silicate, $HfSiO_4$, and is isomorphous with zircon, $ZrSiO_4$. It is not plentiful enough to be considered an ore of Hf; however, there has been recent interest in its physical properties. Oxides with a medium dielectric constant and wide band gap are required to replace SiO_2 as the gate insulator in future complementary metal oxide semiconductor (CMOS) devices. New materials are currently being developed to replace the SiO_2 gate dielectric; however, alloying many of the binary oxides with SiO_2 increases the crystallization temperature of the dielectric at the cost of lowering the dielectric constant (Wilk et al. 2000). One promising candidate is hafnium silicate, $HfSiO_4$, and some of its non-stoichiometric $HfSi_xO_y$ pseudobinary mixtures because the interface between silicon and $HfSiO_4$ is stable against SiO_2 formation (Johnson-Steigelman et al. 2002).

In addition, hafnon and its isomorphs (zircon, thorite, and coffinite) appear to be effective "radiation-resistant" materials suitable for fission-reactor applications (Meldrum et al. 1998) and for use as a waste form for ^{239}Pu resulting from the dismantling of nuclear weapons. In the cascading events that occur during ion radiation, extremely high pressures and temperatures exist in very localized environments for short time periods. For this reason, efforts have been directed toward understanding the thermodynamics and transformations of these materials at high pressure and high temperature (cf. Meldrum et al. 1998, 1999a, 1999b; Rios and Boffa-Ballaran 2003). Most of the research, however, has been focused on zircon.

In the natural state, hafnon ($HfSiO_4$) is always "contaminated" by Zr^{4+} and in some cases by U^{4+}, Th^{4+}, or Y^{3+} (Anthony et al. 1995) and forms a complete chemical solid solution with zircon (Ramakrishnan et al. 1969). Because Hf^{4+} and Zr^{4+} have similar atomic radii, hafnon and zircon "cannot be distinguished by X-ray diffraction" (Anthony et al. 1995). However, Nicola and Rutt (1974) observed significant differences between their Raman spectra due to the large difference in mass between Hf and Zr, and they were able to make some Raman mode assignments. Hoskin and Rodgers (1996) demonstrated a positive correlation between Hf content and frequency of stretching modes. Using Raman spectroscopy, Zhang et al. (2000) (as well as Wopenka et al. 1996; Nasdala et al. 1995, 1996, 1998) showed that the phase changes induced by radiation damage in natural zircon does not result in the bulk chemical dissociation of $ZrSiO_4$ into ZrO_2 and SiO_2.

Hazen and Finger (1979) determined the crystal structure and compressibility of zircon at pressure and concluded that it was the least compressible tetrahedrally coordinated silicate known at the time. Reid and Ringwood (1969) demonstrated that zircon undergoes a phase transformation at elevated temperature and pressure conditions. Using Raman spectroscopy and X-ray diffraction (XRD), Knittle and Williams (1993) reported that zircon undergoes a quenchable phase transition at ~23 ± 1 GPa to the scheelite structure with space group $I4_1/a$, a subgroup of the symmetry of zircon ($I4_1/amd$). The transformed phase is about 10% more dense than zircon. Phase transitions at high pressure and room temperature are usually hampered by sluggish kinetics, prompting Knittle and Williams (1993) to suggest that the transition of zircon displays an anomalous and possibly unique silicate transformation mechanism. Knittle and Williams (1993) used a mixture of methanol, ethanol, and water as a pressure medium, which is frozen and nonhydrostatic above 15 GPa. The zircon

* E-mail: manounb@fiu.edu

0003-004X/06/1112–1888$05.00/DOI: 10.2138/am.2006.2070

transformation also has been observed in shock experiments (Mashimo et al. 1983; Kusaba et al. 1985), and in other diamond anvil studies (Liu 1979; Ono et al. 2004; van Westrenen et al. 2004). The transformed phase subsequently has been found in meteorite impact debris and has been named reidite (Glass et al. 2002). The presence of reidite and its transformation pressure from zircon can be used as a geobarometer. Liu (1979) and more recently Tange and Takahashi (2004) reported that zircon dissociates into ZrO_2 and SiO_2 at pressures higher than 20 GPa and elevated temperatures.

There is, however, some debate on the compressibility of zircon and its transition pressure. The early work on natural samples produced a bulk modulus for zircon of K_o = ~227 ± 2 GPa. However, van Westrenen et al. (2004) used a synthetic sample with a neon pressure medium and obtained a value that is 12% lower, (K_o = 199 ± 1 GPa), and a transformation pressure of 19.7 GPa, which is 3 GPa lower than previous studies. They suggested that the earlier studies were conducted under nonhydrostatic pressure conditions, a small range of investigated pressure, and with a significant Hf content in the zircon. Because the unit-cell volume of Hf is smaller than for zircon, then by the Birch Law it is probable that the bulk modulus of hafnon should be greater than for zircon. This is also consistent with the observation that the Raman stretching frequencies of the Si-O bond for hafnon are greater than for zircon (Nicola and Rutt 1974; Hoskin and Rodgers 1996). Therefore, zircon that contains significant amounts of Hf should have a larger bulk modulus. Ono et al. (2004) obtained a statistically identical bulk modulus (K_o = 205 ± 8 GPa) for a natural zircon that was heated after each pressure increase to reduce the effects of nonhydrostatic conditions in the diamond-anvil cell. Their sample transformed to the reidite phase at ~10 GPa while heating. They did not report the chemistry of their sample.

In this paper, we present the Raman spectra of synthetic, pure $HfSiO_4$ as a function of pressure to 38.2 GPa at room temperature. Because of the similarities in the room condition structures of $ZrSiO_4$ and $HfSiO_4$, we investigated whether a transformation similar to the zircon-to-reidite one also is observed in the hafnium silicate and compare the spectra of the two materials.

Experimental methods

Single crystals of synthetic, pure $HfSiO_4$ hafnon were kindly provided by Alex Speer. The crystal structure of this sample was previously studied by single-crystal XRD (Speer and Cooper 1982) and shown to be extremely well crystallized with cell parameters a = 6.5725 ± 0.0007 Å, c = 5.9632 ± 0.0004 Å, V = 257.597 Å^3, and space group symmetry $I4_1/amd$. In the present study, the sample was ground to a powder with particle sizes of ~3 µm and loaded into a high-pressure diamond-anvil cell (DAC) with 400 µm diameter culets. A T301 steel gasket was used with a sample chamber hole pre-indented to 47 µm in initial thickness and 150 µm in diameter. Ruby chips were loaded with the sample and pressures were determined by the pressure-dependent spectral shift of the sharp ruby fluorescence R1 line (Mao et al. 1986), excited by an argon ion laser with a wavelength of 514.5 nm. Any pressure medium maintains the sample at a high hydrostatic state only at relatively low pressure, but at pressures >15 GPa, the state mostly becomes quasi-hydrostatic due to the solidification of the pressure medium, including liquid and gas. In this study, no pressure medium was employed; however, such a sample loading may lead to a pressure gradient across the sample chamber. Therefore, the focused laser spot on the sample was close to a ruby chip, to ensure that the pressures subjected to the sample and the ruby chips were similar.

Raman spectra were collected in a back-scattering arrangement at room temperature using a high throughput holographic imaging spectrograph with volume transmission grating, holographic notch filter, and thermoelectrically cooled CCD detector (Physics Spectra) with a resolution of 4 cm^{-1}. The spectrometer and Raman spectra were calibrated using the Raman lines of diamond and sulfur as well as the neon emission spectrum. A Ti^{3+}-sapphire laser pumped by an argon ion laser was tuned at 785 nm. The laser power was operated at 100 mW at low pressures and 300 mW at high pressures, and the incident laser beam was focused to a spot size of 5 µm using a 20× objective. Each exposure time was 7 min with 2 accumulations. The total wavenumber range covered was from 180 to 2000 cm^{-1}.

Results and discussion

Speer and Cooper (1982) refined the structure of hafnon, in the tetragonal system with space group $I4_1/amd$, in the second setting, in which the Hf atoms are located on the 4a sites (0, 3/4, 1/8), Si on the 4b sites, and O on the 16h sites. Group theory analysis gives 12 Raman active modes for hafnon, represented as $2A_{1g} + 4B_{1g} + B_{2g} + 5E_g$. Only eight of the modes in the Raman spectrum of hafnon were observed (Fig. 1). Nicola and Rutt (1974) observed two additional modes, at 159 and 148 cm^{-1}. Both of these frequencies are below the wavenumber range that can be detected in this work with our instrumental setup. The Raman vibrational frequencies at ambient pressure with their mode assignments (Syme et al. 1977) are given in Table 1. The modes observed in the region 400–1100 cm^{-1} are internal stretching and bending vibrations of the $(SiO_4)^{4-}$ tetrahedra whereas the modes observed at 351.3 and 214.2 cm^{-1} are external modes. Knittle and Williams (1993) noted that zircon exhibits a high Raman frequency for an SiO-stretching vibration (1006 cm^{-1}), and we point out that this frequency in hafnon (1021.5 cm^{-1}), the $(SiO_4)^{4-}$ antisymmetric stretching vibration, is even higher. The high values of the SiO stretching frequencies in zircon were attributed to coupling with strong ZrO vibrations (Knittle and Williams 1993).

Raman spectra were collected at one atmosphere and at elevated pressures, and are illustrated in Figure 2. The Raman peaks increased in width and became more indistinct with increasing pressure, as is typical for a sample that is examined without a pressure medium. Consequently, only the five most intense modes were followed as a function of pressure. Fitted peak positions for one atmosphere are recorded in Table 1, and plotted in Figure 3. Additional peaks first appear in the spectrum recorded at 20.6 GPa. The pressure derivatives of the peak positions below 20.6 GPa are computed by linear fits and are listed in Table 1. In hafnon, the individual vibrational mode shifts are statistically identical to those of the four corresponding peaks observed in zircon by Knittle and Williams (1993). However, the 214 cm^{-1} peak, which was only measured at ambient conditions in the zircon study, has a negative pressure derivative in hafnon and displays soft mode behavior. Knittle and Williams (1993)

Table 1. Observed Raman modes and their pressure dependences of hafnon, $HfSiO_4$, at room conditions, together with the peak assignments that were made according to Syme et al. (1977)

Frequencies (Δcm^{-1})	dν/dP (cm^{-1}/GPa) hafnon	dν/dP (cm^{-1}/GPa) zircon	Assignment
214.2	–0.5	–	E_g+B_{1g}
351.3	2.7	3.2	E_g
400.2			E_g
450.3	1.1	1.1	A_{1g}
639.5			B_{1g}
934.9			E_g
985.7	4.1	4.1	A_{1g}
1021.5	4.6	4.8	B_{1g}

suggested that there should be an external mode in zircon because the average spectroscopic Grüneisen parameter computed in their study was much larger than estimates of the thermodynamic Grüneisen parameter, and the difference between the two could be resolved if a peak in zircon existed with negative pressure derivative. Nicola and Rutt (1974) assigned the 214 cm^{-1} peak to the E_g libration mode of the SiO_4 group. This mode corresponds to the 201 cm^{-1} line in zircon. In their single-crystal Raman study of the high-pressure transformations of $TbVO_4$ and $DyVO_4$ from the zircon to the scheelite structure, Duclos et al. (1989) observed two soft modes in the zircon-structure phases. One of the soft modes corresponds with the one that we observed in the present study, whereas the other was found at ~150 cm^{-1}, below the wavenumber range detected in the present work. When pressure increases, a negative shift for the peak centered at 214 cm^{-1} was observed. This peak is an overlap of E_g+B_{1g} modes; these modes have different pressure shifts and hence appear to split at high pressures at 14.3 GPa (Fig. 2).

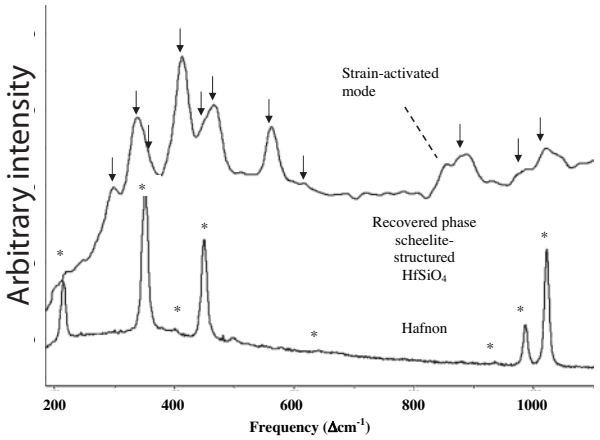

FIGURE 1. Ambient-pressure Raman spectra for $HfSiO_4$ (hafnon structure = *) starting material and for the sample quenched from 38.2 GPa and 300 K, which has converted to the scheelite-structured $HfSiO_4$ phase (arrows). Peak assignments for the two spectra are given in Tables 1 and 2. The high-pressure resulting spectrum is clearly distinct from the spectrum obtained from the hafnon (starting material) and similar to the reidite spectrum decompressed from the zircon phase transformation.

At pressures up to 18.7 GPa, all Raman peaks can be assigned to hafnon. At 20.6 GPa, an additional broad and weak peak appears at ~618 cm^{-1}. Knittle and Williams (1993) also observed the appearance of a similar peak (610 cm^{-1}) at the onset of the zircon-reidite transformation. Another new peak, located at ~510 cm^{-1}, appears on the shoulder of the 450 cm^{-1} peak, and becomes separate and distinct at 34.3 GPa with the frequency 526.2 cm^{-1}. In addition, the two highest frequency vibrations become broad and indistinct with increasing pressure, and cannot be clearly located in the spectrum recorded at ~38.2 GPa. These changes in the Raman spectrum are consistent with the zircon-reidite phase transition previously observed by Knittle and Williams (1993), and indicate the transformation of hafnon to the scheelite-structured $HfSiO_4$. The transformation pressure for hafnon at room temperature is then given as (18.7+20.6)/2 = 19.6 ± 1 GPa. Knittle and Williams (1993) reported that the transformation from zircon to reidite occurred at 23 ± 1 GPa. However, in their XRD study at pressure, van Westrenen et al. (2004) reported a transformation at 19.7 GPa for a synthetic, pure zircon. They suggested that the higher transformation pressure recorded by Knittle and Williams (1993) is a consequence of composition and impurities in their natural sample. It is clear from our study that the Hf content does not increase the transformation pressure.

The vibrational modes of the scheelite-structured $HfSiO_4$ were measured to 38.2 GPa and on decompression. Figure 4 illustrates the Raman spectra during decompression, and pressure shifts of these modes are tabulated in Table 2 and plotted in Figure 5. As illustrated in Figure 4, the low-frequency vibrations decrease continuously on decompression, whereas the high-frequency SiO_4 internal modes are not resolved until pressures below 5.5 GPa are reached, at the same pressure a peak appeared at about 893 cm^{-1}. Upon complete decompression, and especially at low frequencies, several additional peaks are resolved in the spectrum

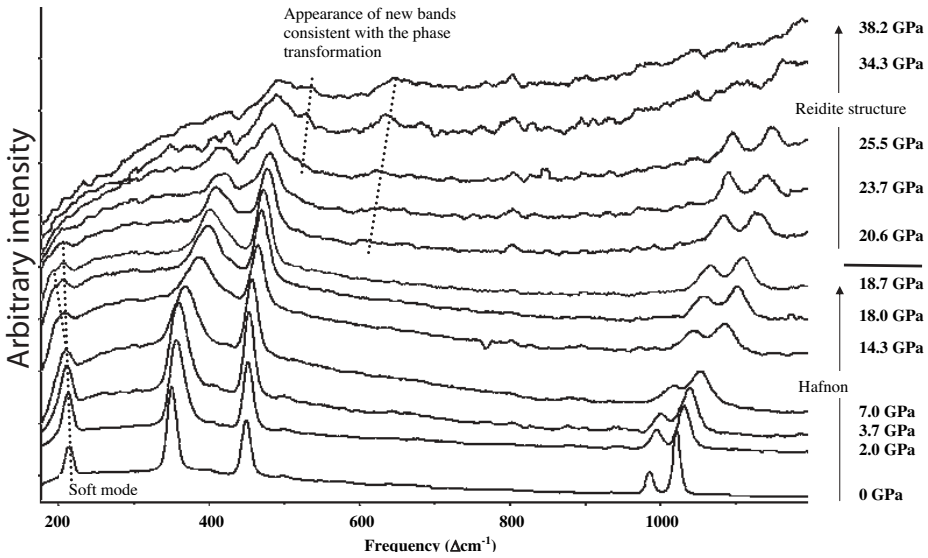

FIGURE 2. Raman spectra through the phase transition from hafnon to scheelite-structured $HfSiO_4$. The spectrum at 20.6 GPa shows the first appearance of a vibration of the scheelite-structured phase at 618 cm^{-1}, and the spectrum at 25.5 GPa shows the appearance of a second peak in the scheelite-structured phase at 525 cm^{-1}. The peak observed at 214 cm^{-1} (1 atm) became undetectable and the 351.3 cm^{-1} peak disappeared after 25.5 GPa.

and appear as weak peaks or shoulders of relatively stronger peaks. Eight modes were observed at 1 atm in $HfSiO_4$ with $I4_1/amd$, in comparison with 11 modes that were observed over the same spectral region in the recovered phase ($I4_1/a$). The in-situ high-pressure Raman study has shown an irreversible phase transition from hafnon to scheelite-structured $HfSiO_4$; note that no hafnon modes were observed upon pressure decrease to ambient conditions, the phase transformation was complete. Group theory analysis predicts 13 Raman active modes arising from the new tetragonal $HfSiO_4$ phase (scheelite-structured $HfSiO_4$), represented as $3A_g + 5B_g + 5E_g$, and 11 modes are observed.

The high-pressure scheelite structure of $HfSiO_4$ is similar to that of the high-pressure structure (reidite) of $ZrSiO_4$, so we assigned the highest frequency Raman vibration in $HfSiO_4$ (scheelite-structured $HfSiO_4$) to the ν_3 antisymmetric stretch (B_g symmetry), with the weak shoulder as the ν_1 symmetric stretch (A_g symmetry). In the 800–900 cm^{-1} region, two peaks appear in the new high-pressure scheelite-structured $HfSiO_4$, although similar compounds with the scheelite structure have only one predicted mode in that region (Vandenborre et al. 1989).

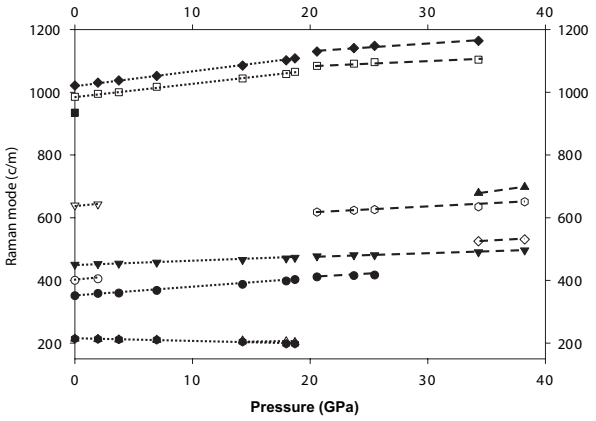

FIGURE 3. Raman frequencies of $HfSiO_4$ as a function of pressure. Up to 18.7 GPa, $HfSiO_4$, has the hafnon structure. The appearance of a new vibrational mode at 618 cm^{-1} at the pressure of 20.6 GPa indicates that the transition to scheelite-structured hafnon has occurred.

Therefore, we assigned the band observed at 884.4 cm^{-1} to the antisymmetric stretch ν_3 (E_g symmetry). The band observed at 853.5 cm^{-1} may be a strain-induced mode, as suggested by Knittle and Williams (1993) and Scott (1968). The peaks observed in the region 420–650 cm^{-1} were assigned to internal SiO_4-bending modes. The external modes are observed at frequencies lower than 420 cm^{-1}.

Comparison of the frequency shifts of the Raman modes suggests that hafnon is more incompressible than zircon (Table 1). Furthermore, the pressure derivatives also suggest that the high-pressure phase of $HfSiO_4$ is more incompressible than reidite ($ZrSiO_4$), which would make it the least compressible tetrahedrally coordinated silicate known at this time. Finally, we notice that the hafnon Raman peaks shift more after the phase transition, which might be due to the

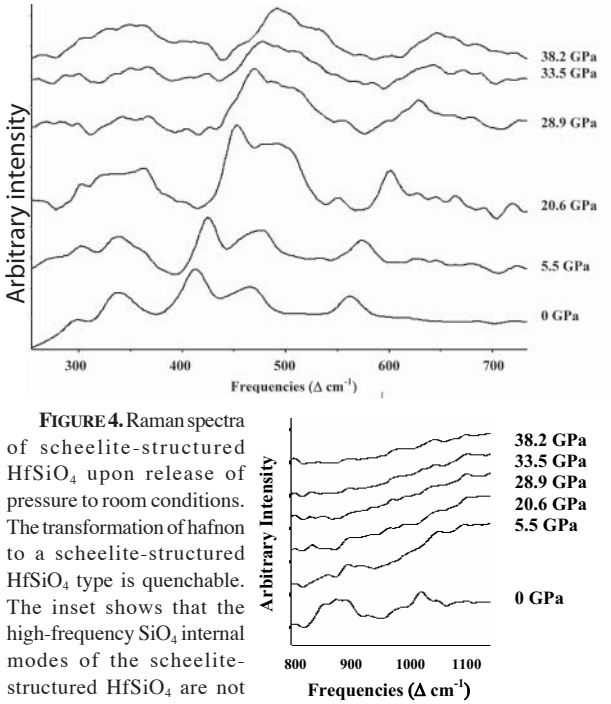

FIGURE 4. Raman spectra of scheelite-structured $HfSiO_4$ upon release of pressure to room conditions. The transformation of hafnon to a scheelite-structured $HfSiO_4$ type is quenchable. The inset shows that the high-frequency SiO_4 internal modes of the scheelite-structured $HfSiO_4$ are not resolved until pressures below 5.5 GPa are reached.

TABLE 2. Observed Raman modes and their pressure dependences of the Scheelite-structured $HfSiO_4$ at room conditions, together with $ZrSiO_4$, reidite (Knittle and Williams 1993)

Frequencies (Δcm^{-1}) Scheelite-structured $HfSiO_4$	dv/d*P* (cm^{-1}/GPa) Scheelite-structured $HfSiO_4$	Frequencies (Δcm^{-1}) $ZrSiO_4$, reidite Knittle and Williams (1993)	dv/d*P* (cm^{-1}/GPa) $ZrSiO_4$, reidite Knittle and Williams (1993)	Assignment Knittle and Williams (1993)
		154		External mode
		196		External mode
		216		External mode
340.4		320		External mode
361		343		External mode
412.4	2.25	392	3.7	External mode
449.1		424	1.5	SiO_4 bend
466.8	1.69	456	2.2	SiO_4 bend
562.1	2.25	552	2.6	SiO_4 bend
618.0		604		SiO_4 bend
853.5		842		Strain-activated mode
884.4	3.57	880	3.7	SiO_4 antisymmetric stretch
981.6		967		SiO_4 symmetric stretch
1019.5	4.32	1001	5.0	SiO_4 antisymmetric stretch

Note: The peak assignments are made according to Knittle and Williams (1993).

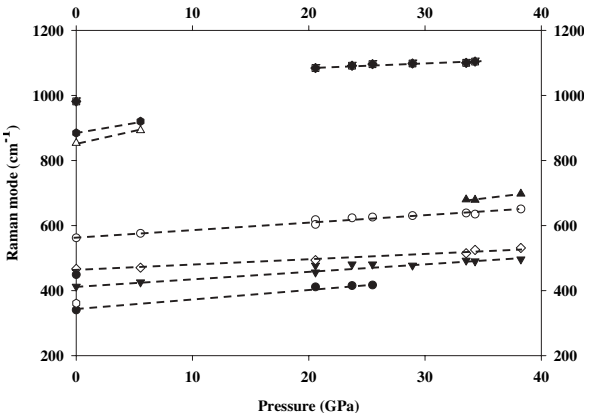

FIGURE 5. Pressure shifts of the vibrational frequencies of scheelite-structured $HfSiO_4$ obtained on compression and decompression. The high-frequency SiO_4 internal modes of the scheelite-structured $HfSiO_4$ are not resolved until pressures below 5.5 GPa are reached.

volume change effects on this mixed phase sample. It is also possible that Raman modes of both phases overlap.

ACKNOWLEDGMENTS

We thank Alex Speer for kindly supplying the samples of synthetic single-crystal hafnon. This work was conducted while R.T.D. was a visiting professor at the Center for the Study of Matter at Extreme Conditions, Florida International University. Surendra Saxena and his colleagues provided an extremely hospitable working environment for which R.T.D. is most grateful. The work is supported by a grant from NSF (DMR 0231291) to S.K.S.

REFERENCES CITED

Anthony, J.W., Bideaux, R.A., Bladh, K.W., and Nichols, M.C. (1995) Handbook of Mineralogy, vol. II, Silica, Silicates, 904 p. Mineral Data Publishing, Tucson, Arizona.

Duclos, S.J., Jayaraman, A., Espinosa, G.P., Cooper, A.S., and Maines, R.G., Jr. (1989) Raman and optical absorption studies of the pressure-induced zircon to scheelite structure transformation in $TbVO_4$ and $DyVO_4$. Journal of Physics and Chemistry of Solids, 50, 769–775.

Glass, B.P., Liu, S.B., and Leavens, P.B. (2002) Reidite: An impact-produced high-pressure polymorph of zircon found in marine sediments. American Mineralogist, 87, 562–565.

Hazen, R.M. and Finger, L.W. (1979) Crystal-structure and compressibility of zircon at high-pressure. American Mineralogist, 64, 196–201.

Hoskin, P.W.O. and Rodgers, K.A. (1996) Raman spectral shift in the isomorphous series $(Zr_{1-x}Hf_x)SiO_4$. European Journal of Solid State and Inorganic Chemistry, 33, 1111–1121.

Johnson-Steigelman, H.T., Brinck, A.V., and Lyman, P.F. (2002) Production of a hafnium silicate dielectric layer for use as a gate oxide by solid-state reaction. Condensed Matter, 0202328 (http://www.arxiv.org/).

Knittle, E. and Williams, Q. (1993) High-pressure Raman spectroscopy of $ZrSiO_4$: Observation of the zircon to scheelite transition at 300 K. American Mineralogist, 78, 245–252.

Kusaba, K., Syono, Y., Kikuchi, M., and Fukuoka, K. (1985) Shock behavior of zircon: Phase transition to scheelite structure and decomposition. Earth and Planetary Letters, 72, 433–439.

Liu, L.G. (1979) High-pressure transformations in baddeleyite and zircon, with geophysical implications. Earth and Planetary Letters, 44, 390–396.

Mao, H.K., Xu, J., and Bell, P.M. (1986) Calibration of the ruby pressure gauge to 800 Kbar under quasihydrostatic conditions. Journal of Geophysical Research, 91, 4673–4676.

Mashimo, T., Nagayama, K., and Sawaoka, A. (1983) Shock compression of zirconia ZrO_2 and zircon $ZrSiO_4$ in the pressure range up to 150 GPa. Physics and Chemistry of Minerals, 9, 237–247.

Meldrum, A., Zinkle, S.J., Boatner, L.A., and Ewing, R.C. (1998) A transient liquid-like phase in the displacement cascades of zircon, hafnon, and thorite. Nature, 395, 56–58.

Meldrum, A., Boatner, L.A., Zinkle, S.J., Wang, S.X., Wang, L.M., and Ewing, R.C. (1999a) Effects of dose rate and temperature on the crystalline-to-metamict transformation in the ABO_4 orthosilicates. Canadian Mineralogist, 37, 207–221.

Meldrum, A., Zinkle, S.J., Boatner, L.A., and Ewing, R.C. (1999b) Heavy-ion irradiation effects in the ABO_4 orthosilicates: Decomposition, amorphization, and recrystallization. Physical Review B, 59, 3981–3992.

Nasdala, L., Wolf, D., and Irmer, G. (1995) The degree of metamictization in zircon: a Raman spectroscopic study. European Journal of Mineralogy, 7, 471–478.

Nasdala, L., Pidgeon, R.T., and Wolf, D. (1996) Heterogenous metamictization of zircon on a microscale, Geochimica et Cosmochimica Acta, 60, 1091.

Nasdala, L., Pidgeon, R.T., Wolf, D., and Irmer, G. (1998) Metamictization and U-Pb isotopic discordance in single zircons: a combined Raman mircoprobe and SHRIMP ion probe study. Mineralogy and Petrology, 62, 1–27.

Nicola, J.H. and Rutt, H.N. (1974) Comparative study of zircon ($ZrSiO_4$) and hafnon ($HfSiO_4$) Raman-spectra. Journal of Physics C: Solid State Physics, 7, 1381–1386.

Ono, S., Tange, Y., Katayama, I., and Kikegawa, T. (2004) Equations of state in $ZrSiO_4$ phases in the upper mantle. American Mineralogist, 89, 185–188.

Ramakrishnan, S.S, Gokhale, K.V.G.K., and Subbarao, E.C. (1969) Solid solubility in the system zircon–hafnon. Materials Research Bulletin, 4, 323–328.

Reid, A.F. and Ringwood, A.E. (1969) Newly observed high-pressure transformations in Mn_3O_4, $CaAl_2O_4$, and $ZrSiO_4$. Earth and Planetary Science Letters, 6, 205–208.

Rios, S. and Boffa-Ballaran, T. (2003) Microstructure of radiation-damaged zircon under pressure. Journal of Applied Crystallography, 36, 1006–1012.

Scott, H.P., Williams, Q., and Knittle, E. (2002) Ultralow Compressibility Silicate without Highly Coordinated Silicon. Physical Review Letters, 88, 015506/1–015506/4.

Scott, J.F. (1968) Lattice perturbations in $CaWO_4$ and $CaMoO_4$. Journal of Chemical Physics, 48, 874–876.

Speer, J.A. and Cooper, B.J. (1982) Crystal structure of synthetic hafnon, $HfSiO_4$, comparison with zircon and the actinide orthosilicates. American Mineralogist, 67, 804–808.

Syme, R.W.G., Lockwood, D.J., and Kerr, H.J. (1977) Raman spectrum of synthetic zircon ($ZrSiO_4$) and thorite ($ThSiO_4$). Journal of Physics C: Solid State Physics, 10, 1335–1348.

Tange, Y. and Takahashi, E. (2004) Stability of the high-pressure polymorph of zircon ($ZrSiO_4$) in the deep mantle. Physics of the Earth and Planetary Interior, 143–144, 223–229.

van Westrenen, W., Frank, M.R., Hanchar, J.M., Fei, Y., Finch, R.J., and Zha, C-S. (2004) In situ determination of the compressibility of synthetic pure zircon ($ZrSiO_4$) and the onset of the zircon-reidite phase transition. American Mineralogist 89, 197–203.

Vandenborre, M.T., Michel, D., and Ennaciri, A. (1989) Vibrational spectra and force fields of scheelite-type germinates. Spectrochemica Acta, 45A, 721–727.

Wilk, G.D., Wallace, R.M., and Anthony, J.M. (2000) Hafnium and Zirconium Silicates for Advanced Gate Dielectrics. Journal of Applied Physics, 87, 484–492.

Wopenka, B., Jolliff, B.L., Zinner, E., and Kremser, D.T. (1996) Trace element zoning and incipient metamictization in a lunar zircon; application of three microprobe techniques. American Mineralogist, 81, 902–912.

Zhang, M., Salje, E.K.H., Farnan, I., Graeme-Barber, A., Daniel, P., Ewing, R.C., Clark, A.M., and Leroux, H. (2000) Metamictization of zircon: Raman spectroscopic study. Journal of Physics: Condensed Matter, 12, 1915–1925.

MANUSCRIPT RECEIVED AUGUST 24, 2005
MANUSCRIPT ACCEPTED MAY 2, 2006
MANUSCRIPT HANDLED BY BRIGITTE WOPENKA